Eur. Phys. J. A 6, 149–155 (1999)

THE EUROPEAN
PHYSICAL JOURNAL A

g-factors in the ground state and in the γ-bands in ^{160,162,164}Dy

F. Brandolini[1], M. De Poli[2], P. Pavan[1], R.V. Ribas[3], D. Bazzacco[1], C.R. Rossi-Alvarez[1]

[1] Dipartimento di Fisica dell'Universita di Padova and Sezione di Padova, INFN, Padova, Italy
[2] Laboratori Nazionali di Legnaro - INFN, Legnaro, Italy
[3] Univ. de S. Paulo, Inst. de Física, Lab. Pelletron - C.P. 66318, S. Paulo, Brazil

Received: 23 March 1999 / Revised version: 14 July 1999
Communicated by C. Signorini

Abstract. The g-factors of some members of the ground state band and of the 2^+ state in the γ-vibrational band have been measured in ^{160,162,164}Dy using the Coulomb Excitation Transient Field technique, induced by ^{58}Ni projectiles at 230, 210 and 217 MeV, respectively. The g-factors in the ground state band are consistent with a constant value, while that of the 2^+_γ states is about 20% larger in average than those in the ground state band. Results are discussed in the frame of the systematics in this nuclear region.

PACS. 21.10.Ky Electromagnetic – 25.70.De Coulomb excitation – 27.70.+q $150 \leq A \leq 189$

1 Introduction

The measurement of g-factors of excited levels in even-even deformed rare earths is of considerable interest, both along the ground state (g)-band, and in the γ-band, since available experimental data are not satisfactory for a close comparison with theoretical predictions [1].

In a pioneer work in ^{158}Dy [2], it has been found that the band crossing of the g-band with the side band, having two aligned neutrons $i_{13/2}$, gives rise to a drastic reduction of the g-factor values. A long standing problem is, however, if the g-factor values along the g-band do experience a reduction already at low spin or just in proximity of the band crossing. In a recent measurement in ^{164,166,168}Er, using the Coulomb Excitation Transient Field (CETF) technique, we obtained nearly constant g-factor values along the g-band up to I=10^+ [3]. Nearly constant values along the g-band up to I=10^+ are consistently predicted by recent theoretical calculations [4,5].

In the same experiment, a larger g-factor value for the 2^+ head of γ-band than that in the ground band was moreover found: in average g_γ/g_g=1.25 [3]. Assuming a strongly coupled rotational model, the g-factor values were found to be in agreement with the angular correlation data in ^{166}Er [6], with γ-branching ratios [7,8] and electron conversion coefficients [9], thus obtaining a fully coherent understanding. We have to note that these results are in disagreement with the 20% reduction of the g-factor value observed at the yrast 6^+ level in ^{166}Er in a Implantation Perturbed Angular Correlation (IMPAC) measurement [10], using the static hyperfine magnetic field.

In the present paper we extend a similar investigation to ^{160,162,164}Dy. Dy stable isotopes have gross properties similar to those of Er and hence similar g-factor values are expected. On the contrary, in a recent IMPAC measurement in ^{160}Dy, the Bonn group found a $\simeq$ 20% reduced g-factor for the yrast 6^+ state [11]. A similar reduction has been reported in ^{164}Dy to occurs already at I=4^+ [12]. Referring to the γ-band, a g_γ/g_g ratio of 0.82(3) has been reported in ^{160}Dy [13], which substantially differs from values found in Er isotopes. As the mentioned Bonn group values are not compatible with the ones obtained in Er isotopes, we considered it worthwhile to check the situation further with a CETF experiment. Some preliminary data in ^{162}Dy and ^{164}Dy were previously communicated at a conference [14].

2 Experimental procedure

The states under study were populated using Coulomb excitation induced by a ^{58}Ni beam at the LNL XTU Tandem. The full experiment required about 6 days of beam on target, using a current of 2-4 pnA. The target consisted of three main layers: the proper target, the ferromagnetic layer of Gd and a metallic backing. The foils were attached to each other with a thin (0.2 mg/cm^2) layer of In. In Table 1, a summary of the experimental conditions is reported. Gd was used as the ferromagnetic layer, since it gives rise to a precession effect about twice as large as the one obtained using iron, but it had to be kept at liquid nitrogen temperature in order to obtain the full magnetization. In order to avoid overlapping of the lines from the excitation of the Gd nuclei, Gd enriched material was used. A metallic sample was obtained by reducing Gd oxide and subsequently rolling to the desired thickness. The Gd foils were annealed following the procedures described in [15]. The magnetization was checked with a double coil

Table 1. Targets used in the experiments

Target Id.	Isotopes	Target (mg/cm^2)	Ferromagnet	thickness (mg/cm^2)	backing (mg/cm^2)	Beam energy (MeV)
1	^{160}Dy	1.5	^{160}Gd	5.8	25 Ag	230
2	^{162}Dy	1.5	^{156}Gd	5.6	25 Ag	210
3	^{164}Dy	1.5	^{156}Gd	5.4	25 Cu	217

magnetometer, and foils were selected having a magnetization better than 6.2 $\mu_\circ$/atom. The external polarizing field, of about 0.03 T, was periodically inverted every few minutes. The backscattered projectiles were registered with a 4x8 cm Parallel Plate Avalanche Counter at 3.2 cm from the target, covering a 2 sr solid angle. The thickness of the Gd layers was chosen such that the exit velocity of the recoil nuclei was larger than about $2v_0$ ($v_0 = c/137$) in order to avoid stopping in the ferromagnetic layer. The experimental conditions for the study of ^{160}Dy ^{162}Dy and ^{164}Dy were different in some secondary aspects.

In the case of ^{164}Dy, four Ge detectors were located at ±64° and ±116°. In the ^{162}Dy measurement the Ge detectors were located at ±65° and ±115°. In both cases four Ge detectors with 25% efficiency were employed and 4μm Mylar foil in front of the particle detector served to stop most of the nuclei backscattered from the target backing.

In the ^{160}Dy measurement the Ge angles were ±68° and ±112° and the Ge detectors had an efficiency of about 80%. It must moreover be noted that in this case, the enrichment of the target material was of only 67% while that for the ^{162,164}Dy targets was about 98%. The thickness of the mylar absorber was increased to 6 μm. Furthermore, in order to enhance the relative efficiency of the $2^+_\gamma \rightarrow 0^+$ transition, a 2 mm thick Pb absorber was positioned in front of the Ge detectors.

The perturbed angular correlation effect is defined according to the formula $\epsilon = (\sqrt{\rho}-1)/(\sqrt{\rho}+1)$ where ρ is the ratio of the coincidence rate in a given detector with the applied field in "up" and "down" direction of the external magnetic field.

The effect in the case of a single excitation is related to the precession angle by the relation $\epsilon = S\Delta\Theta$, where S is the logarithmic derivative of the angular correlation. In the present case the cascading population had to be taken into account.

The experimental slope S has been checked by measuring the effect obtained with the magnetic field fixed in one direction and rotating the Ge assembly by ±3°. This was the maximum angle for which no variation of γ-ray absorption was assured in our experimental setup.

3 Experimental results and data analysis

An example of coincidence γ-ray spectra at forward angles for the three reactions is shown in Fig. 1. The measured effects are shown in Table 2. In the same Table, the calculated slopes and direct population fractions P_{dir} are also reported, provided by the code COULEX [16].

Table 2. Experimental effects, calculated slopes and percentage of direct populations (see text)

Nucleus	I^π	$\epsilon(^o/_{oo})$	$S_{calc.}$	P_{dir}
^{160}Dy	6^+	45.0(11)	0.770	48
	8^+	39.1(13)	0.721	74
	10^+	30.0(23)	0.690	85
	12^+	31.0(60)	0.682	95
	2^+_γ	201.1(120)	3.390	100
^{162}Dy	6^+	48.6(9)	0.778	50
	8^+	43.8(14)	0.740	76
	10^+	34.3(35)	0.710	89
	2^+_γ	198.0(130)	2.626	100
^{164}Dy	6^+	38.0(8)	0.775	43
	8^+	33.0(10)	0.738	67
	10^+	30.0(20)	0.711	81
	2^+_γ	146.0(100)	2.408	100

Predictions of the code COULEX have been universally recognized to be highly reliable. The code includes an internal control which check whether a safe bombarding energy is used, to avoid nuclear reaction competition and thus in order to guarantee a calculation precision of few percent. Our bombarding energies were in every case in safe conditions. To give an example, the classical Coulomb barrier for the collision of ^{58}Ni ions on ^{160}Dy is 324 MeV, while the safe energy evaluated by COULEX is 232 MeV.

Theoretical slopes have been adopted, owing to their high reliability, while slope measurements were performed mainly as an apparatus check. In this respect it has to be noted that the effects corresponding to the rotation of the γ-detector assembly by an angle of 3° were smaller than the experimental effects caused by the precession of the TF perturbed angular correlations. For a precise determination of S(θ), much longer experimental runs would have been required in order to get an adequate accuracy in the determined g-factors.

The uncertainty to apply to the calculated slopes is mainly related with the choiche of the matrix elements, since the geometry of the particle detector has been precisely taken into account, as in previous papers [15,3]. Calculated values in Table 2 were obtained using symmetric rotor model matrix elements and including the γ-band. Since some triaxiality ($\gamma \simeq 0.10$) could not be excluded, similarly to the case of ^{166}Er [17] a comparison was also made with the triaxial rotor-vibration model. Predictions

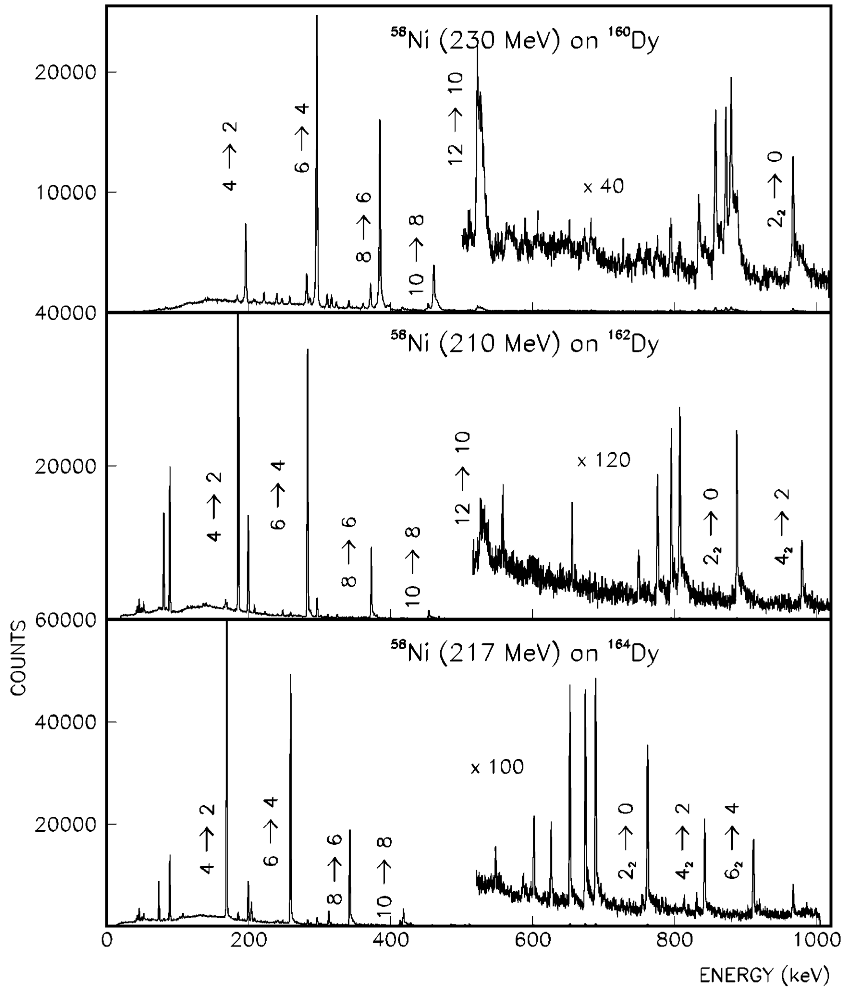

Fig. 1. Typical coincidence γ-ray spectrum taken at +68° +65°, +64° in the ^{160}Dy, ^{162}Dy and ^{164}Dy measurements, respectively

change sensibly below the 4^+ state, but, on the other hand, in the present work we are not dealing with the yrast 2^+ and 4^+ states, since they are mainly populated indirectly from upper levels and their experimental intensity could not be determined precisely, owing to the low energy. For the levels of interest the calculated slopes were stable well within 5%, while the P_{dir} values within 10 %.

An insidious source of systematic errors could be represented by a detachment of the target layers which would result both in a reduction of gamma anisotropy due to vacuum deorientation and in a change of the angular precession. The presence of a gap between the layers was efficiently monitored by the line shape of the γ-transitions.

The precession data were analyzed with the MAGMO code [18], which simultaneously fits all the γ-transitions in several independent measurements, having the g-factors of the relevant levels as free parameters. Both the multiple Coulomb excitation in the given experimental geometry, using COULEX as subroutine, and the complex decay of the set of levels are handled by the code. In order to describe the transient field in Gd, the Chalk River (CR) parameterization [19,3] $B_{TF} = 27.5 v/v_0 Z \exp(-0.135 v/v_0)(kT)$ is employed by the program.

In our previous CETF measurement in rare earths using Gd as ferromagnet [14,3,20] it turned out that the CR parameterization works well if the foils are carefully prepared according the recipe of [15].

The deduced g-factors are reported in Table 3, where the errors do not include the calibration contribution, which we estimate to be less than 15 %. Such contribution accounts of the uncertainty in the determination of magnetization and target thickness of our targets (typically 5%), as well as of the uncertainty in the CR parameterization [19]. The quoted uncertainty is mostly related to the field normalization, so that it affects little the g-factor comparison in the same isotope.

4 Discussion

4.1 The g-band

In order to get the well known value of the g-factor of the 2^+ state as internal reference, and thus to extend the CETF experiment to include the $2^+ \rightarrow 0^+$ transition, a delicate and time consuming set of measurements

Table 3. Summary of experimental g-factors

Nucleus	I^{π}	E_{γ} keV	halflife (ps)	adopted$^{a)}$	Bonn $^{b)}$	Canberra$^{c)}$
^{160}Dy	2^+	86.8	2020(10)	0.362(9)		
	4^+	197.0	103(5)		0.359(30)	
	6^+	297.2	18.6(10)	0.352(17)	0.242(20)	
	8^+	385.7	3.43(25)	0.343(22)	0.301(95)	
	10^+	461.9	1.56(7)	0.306(31)		
	12^+	522.8	0.89(4)	0.302(60)		
	2^+_{γ}	966.2	1.31(9)	0.401(27)	0.317(12)	
^{162}Dy	2^+	80.1	2200(30)	0.343(12)		
	4^+	185.0	132(5)		0.285(31)	
	6^+	282.9	18.4(10)	0.364(18)	0.301(31)	
	8^+	372.4	4.2(2)	0.381(20)	0.429(123)	
	10^+	453.8	1.57(10)	0.364(35)		
	2^+_{γ}	888.2	1.98(10)	0.460(30)		
^{164}Dy	2^+	73.4	2380(30)	0.342(12)		
	4^+	168.8	200(10)		0.251(31)	
	6^+	259.1	26.6(10)	0.325(17)	0.272(50)	0.28(8)
	8^+	342.3	7.2(5)	0.310(20)		0.27(9)
	10^+	417.6	2.3(2)	0.311(35)		0.35(13)
	2^+_{γ}	761.8	4.6(3)	0.382(27)		0.31(10)

a) Present work, apart for 2^+ level data [24]. Calibration uncertainty is not included.
b) Ref. [11], apart for ^{164}Dy data [12] and 2^+_{γ} state in ^{160}Dy [13].
c) Ref. [32].

at different bombarding energies, using a thin Gd layer, would have been necessary which was not exploited in the present case. This was done for ^{156}Gd [21], where the g(4^+)/g(2^+)=0.84(6) ratio reported in [22,23] was disproved. Since in the present case we measured each isotope at one bombarding energy, we have to rely on the TF calibration, thus getting a lower precision, but still sufficient to draw some conclusions.

In Table 3 we have assumed the 2^+ g-factor values from the compilation of [24], which substantially agrees with [1]. We note that for ^{160}Dy we assume 0.362(9), while in [11] 0.385(6) is used. We preferred the former choice, which only marginally affects the discussion, because the latter implies a static field value correlated with some g-factor values we are comparing. We note that the reported 2^+ g-factor and the 6^+ value agree within the given accuracy of 10%.

For a better comparison, the obtained data are shown in Fig. 2. Yrast bands are known to be very regular in ^{162}Dy and ^{164}Dy up to I=14^+, so that rotational g factor values are expected along the band, as experimentally observed. The situation in ^{160}Dy is different, as an up bending starting around 12^+ suggests a mixing with a sideband due to the alignment of two neutron $i_{13/2}$. The g-factor values are expected to decrease approaching I=12^+, as it appears to occur experimentally. In the same figure a comparison with recent theoretical calculations is reported. The most reliable theoretical calculations are probably those using the angular momentum projected shell model (AMPSM) [25], which predict rather well the crossing of the g-band with the two-neutron aligned band in Dy isotopes. The absolute value of the g-factors is well reproduced, as it was for Er isotopes [3]. The somewhat too low value in ^{164}Dy is consistent with the quoted calibration uncertainty.

The influence of neutron alignment was predicted to be negligible in cranked Hartree-Fock-Bogoliubov (CHFB) calculations [26], where constant values were found. Other CHFB calculations were made in [27], where a small decrease is reported (∼6% at 6^+), when using Nilsson parameters [28]. These data are not represented in Fig. 2 since only relative values are available. Furthermore, older calculations in ^{164}Dy predicted a constant behavior [29]. The same figure shows a relevant disagreement between our data and those of the Bonn group. In the case of ^{160}Dy they report g(6^+)/g(4^+)= 0.67(4), without correlation with anomalies in the rotational band spacings. The disagreement would be even bigger if one assumes in the present experiment an incomplete magnetization, caused by imperfect annealing. It is also difficult to explain the ratio g(4^+)/g(2^+)= 0.73(9) in ^{164}Dy [12], that proposes an anomaly similar to the one, not confirmed, in ^{156}Gd [22]. The value could not be checked in the present measurement because of the low sensitivity. As mentioned before, theories predict in every case a smooth decrease with increasing spin, so that the measured g factor reduction at I= 4^+ should also reflect in a reduction at I=6^+, which was not observed. In order to accommodate this discrepancy, in [12] it has been even argued that, along the g-

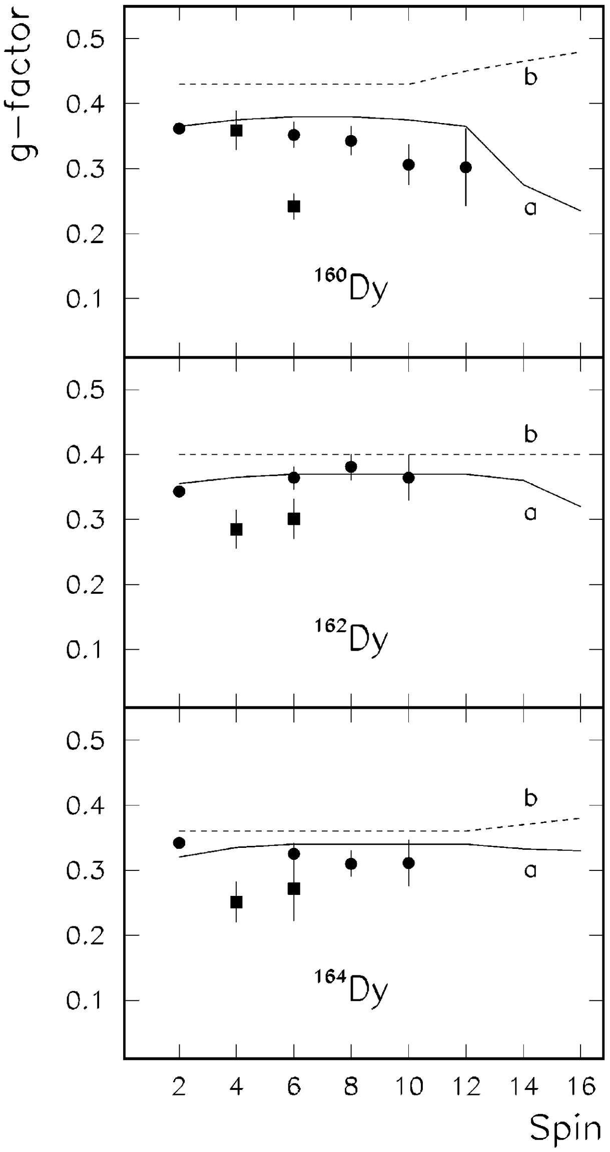

Fig. 2. Spin-dependence of the g-factor values for yrast levels in ^{160}Dy, ^{162}Dy and ^{164}Dy, respectively. Adopted experimental values are shown by full circles while Bonn data by full squares (8^+ states data are not reported, owing to the very large error bar). Theoretical curves were obtained with a) AMPSM [25], b) CHFB [26], respectively

band, the reduction could oscillate with increasing spin, in contrast with any theoretical calculations. In the same reference it has been furthermore argued that our CETF measurements [3] could be incorrect due to the use of too thick Gd layer, which would cause a fraction of decaying nuclei to experience the large static field in Gd ($\simeq$ 440T in Gd). This case can be excluded in the present and in the previous experiments. The thickness was chosen to a large degree of safety and MonteCarlo simulations exclude any stopping in Gd. For this purpose a version of the MonteCarlo code LINESHAPE [30] was used, adapted to Coulomb Excitation reactions for a recent stopping power study [31].

4.2 The $\gamma-$band

The ratio $g(2^+_\gamma)/g(6^+_g)$ determined in the present work is 1.14(9), 1.26(10) and 1.17(10) for ^{160,162,164}Dy respectively. Assuming that g(6^+) is equal to g(2^+) within some percent, as discussed in the previous section, a significant variation of the g-factor of the 2^+_γ-vibrational states relative to the one of the g-band is clearly evidenced. In ^{160}Dy our value of g_γ/g_g of 1.14(9) disagrees with that of 0.82(3) recently reported [6]. Previously the $g(2^+_\gamma)/g(6^+_g)$ value for ^{164}Dy was reported to be 1.12(18) [32], which is not conclusive, owing to the large error.

Our experimental values of g_γ/g_g in Dy isotopes are similar to the ones in Er isotopes [3], therefore one can draw similar conclusions. When comparing with the strongly coupled rotational model formula for g-factors:

$$g = g_R + (g_K - g_R)K^2/I(I+1)$$

one derives the values ($g_K - g_R$)= 0.06(4), 0.14(5), 0.11(5), for ^{160,162,164}Dy respectively.

In ^{162}Dy, the obtained value of $g_K - g_R$ can be compared with that deduced from the rotational formula for the $\gamma-$transitions [7]:

$$|g_K - g_R| = \frac{0.93 \cdot E_\gamma \cdot |Q_\circ|}{|\delta|\sqrt{(I-1)(I+1)}}$$

By inserting the known values of $|\delta|$ for the $4^+ \rightarrow 3^+$ and $5^+ \rightarrow 4^+$ intra-band transitions in the γ-band [8], deduced from intensities measurements, and taking $Q_\circ$=7.28(10)eb [33] and E_γ =0.888 MeV the value $|g_K - g_R|$=0.08(4) is deduced, which is consistent with present data. The present present experiment thus give a further support to the picture outlined for Er isotopes [3] even if the comparison is not equally complete. In particular experimental mixing values δ, which would allow to get the sign of the $g_K - g_R$ value, are not available.

The Geometrical Collective model (GCM) [34,9], based on a different deformation of the proton and neutron fluids caused by the pairing force, predicts in both Dy and Er isotopes mixing ratios consistent with experiments. It predicts, however, a rather too small g_γ/g_g ratio of 1.06 [9].

Another important collective model is the interacting boson one (IBM). In its IBM2 version, which considers protons and neutrons separately, a variation of the g_γ/g_g ratio from unity is to be related to F-spin impurity [35]. According to that reference, which adopt the same sign convention as Nuclear Data Sheets [36] a positive sign is necessary for the mixing ratio in the inter-band transitions in order to account for the observed g_γ/g_g ratio. Experimentally, negative values are often reported, but it must be noted that experimental data are affected by large errors and even the sign convention is not always sure, so that it would be of worth to re measure them.

Microscopical calculations could account for the intrinsic composition of the wave functions in the γ-band and thus of its g-factor values. Such calculations have been so far not reported in the literature, but they are planned to be performed with AMPSM [37].

5 Summary

Our data for Dy stable even-mass isotopes confirm what was previously found in the Er ones: i.e., fairly constant g-factor values along the g-band and somewhat bigger g-factor values for the 2^+_γ states.

Our conclusions substantially differ from those of the Bonn group. Their data disagree, however, also with the more reliable theoretical predictions, so that the possibility that they are affected by a persisting systematic error is a realistic possibility. It may be that the dynamics of the building-up of hyperfine static fields is not yet fully understood.

Present data are affected by a rather large error bar, which prevents from investigating any fine structure. For this purpose a new experiment with higher statistics would be of interest.

After the first submission of this paper we became aware of two papers in press, which confirm our conclusions: 1) further AMPSM calculations were done in ^{160,162,164}Dy, which reproduce better the backbending, when leaving g-factor values nearly unchanged [38]. 2) A possible explanation has been given very recently [39] of the dropping down of the g-factor values at low spin in the g-band, when extracted from in-beam IMPAC measurements. It may be caused by a thermal spike during the first 5-10 ps after implantation, when the local temperature is higher than the Curie one and thus the hyperfine static magnetic field in Gd is not active.

Thanks are due to D.R. Napoli, as well as to M. Ionescu-Bujor and C. Fahlander, for several collaborative discussions. We are grateful to A. Buscemi, S. Martini and R. Zanon for the help on the experiment preparation, to dr. R. Pengo and G. Manente for contribution to the target preparation. R.V. R. would like to acknowledge financial support from the Brazilian agency CNPq (Conselho Nacional de Desenvolvimento Científico e Tecnológico) and the Italian INFN (Istituto Nazionale di Fisica Nucleare).

References

1. Table of Isotopes-eighth edition, R.B. Firestone and V.S. Shirley editors (J. Wiley and Son 1996), Appendix E
2. G. Seiler-Clark, D. Pelte, H. Emling, A. Balanda, H. Grein, E. Grosse, K. Kulessa, D. Schwalm, W.J. Wollersheim, H. Hass, G.J. Kumbartzki and K.H. Speidel, Nucl. Phys. **399**, 211 (1983)
3. F. Brandolini, C. Cattaneo, R.V.Ribas, D.Bazzacco, M. De Poli, M. Ionescu-Bujor, P. Pavan, C. Rossi Alvarez, Nucl. Phys. A**600**, 272 (1996)
4. K. Hara, Y. Sun, Int. J. Mod. Phys. E **4**, 637 (1995)
5. K. Sugawara-Tanabe, K. Tanabe, Phys. Lett. B **207**, 1243 (1988)
6. I. Alfter, E. Bodenstedt, W. Knichel, J. Schüth, Z.Phys. A **355**, 277 (1996)
7. C.W. Reich and J.E. Cline, Nucl. Phys. A **159**, 181 (1970)
8. W. Gelletly, W.F. Davidson, J. Simic, H.G. Borner, A.F. Diggory, W. Mampe, K. Schreckenbach, D.D. Warner, J. Phys. G **4**, 575 (1978)
9. K. Schreckenbach and W. Gelletly, Phys. Lett. B **94**, 298 (1980)
10. A. Alzner, E. Bodenstedt, B. Gemünden, J. van den Hoff and H. Reif, Z. Phys. A **322**, 467 (1985)
11. I. Alfter, E. Bodenstedt, W. Knichel, J. Schüth, Z. Phys. A 357, **13** (1997)
12. I. Alfter, E. Bodenstedt, W. Knichel, J. Schüth, H. Grawe Hyperfine Inter. **110**, 313 (1997)
13. I. Alfter, E. Bodenstedt, W. Knichel, J. Schüth, Z. Phys. A **353**, 17 (1995)
14. F. Brandolini, in *Proceedings of the Conference on Perspectives for the Interacting Boson Model*, edited by R.F. Casten, A. Vitturi, A.B. Balantiken, B.R. Barrett, J.N. Ginocchio, G. Maino, and T. Otsuka. (World Scientific, 1995) p. 647
15. F. Brandolini, P. Pavan, D. Bazzacco, C. Rossi Alvarez, R.V. Ribas, M. De Poli and A.M.I. Haque, Phys. Rev. C **45**, 1549 (1992)
16. A. Winther and J. De Boer, in: *Coulomb Excitation*, eds. K. Alder and A. Winther (Academic, 1966), p. 303
17. C. Fahlander, I. Thorslund, B. Varnestig, A. Bäcklin, L. E. Svensson, D. Disdier, L. Kraus, I. Linck, N. Schulz, J. Pedersen, D. Cline, Nucl. Phys. A **537**, 183 (1992)
18. R.V. Ribas, Nucl. Inst. Meth. Phys. Res. A **328**, 553 (1993)
19. O. Häusser, H.R. Andrews, D. Horn, M.A. Lone, P. Taras, P. Skensved, R.M. Diamond, M.A. Deleplanque, E.L. Dines, A.O. Macchiavelli, F.S. Stephens, Nucl. Phys. A **412**, 141 (1984)
20. D. Bazzacco, F. Brandolini, K. Löwenich, P. Pavan, C. Rossi Alvarez, M. De Poli, and A.M.I. Haque Hyperfine Interact. **59**, 133 (1990)
21. D. Bazzacco, F. Brandolini, K. Löwenich, P. Pavan, C. Rossi Alvarez, M. De Poli, and A.M.I. Haque, Hyperfine Interact. **59**, 125 (1990)
22. A. Alzner, E. Bodenstedt, B. Gemünden, J. van der Hoff, S. Piel, R. Sajok, Th. Schäfer, R. Vianden, Z. Phys. A **331**, 277 (1988)
23. Th. Schäfer, R. Vianden and E. Bodenstedt Z. Phys. A **335**, 387 (1990)
24. A. E. Stuchbery, Nucl. Phys. A **589**, 222 (1995)
25. Y. Sun and J.L. Egido, Nucl. Phys. A **580**, 1 (1994)
26. M. L. Cescato, Y. Sun and P. Ring, Nucl. Phys. A **533**, 455 (1991)
27. M. Saha and S. Sen, Nucl. Phys. A **552**, 37 (1993)
28. S.G. Nilsson, C.F. Tsang, A. Subiczewski, Z. Szymanski, S. Wycech, C. Gustafson, I.L. Lamm, P. Möller and B. Nilsson, Nucl. Phys. A **131**, 1 (1969)
29. M. Diebel, A.N. Mantri, U. Mosel, Nucl. Phys. A **345**, 72 (1980)
30. J. C. Wells and N. Johnson. Report No. ORNL-6689, 1991, p. 44 (unpublished)
31. F. Brandolini, N.H. Medina, M. De Poli, P. Pavan, M. Wilhelm, A. Dewald and G. Pascovici, Nucl. Instr. and Meth. B **132**, 11 (1997)

32. C.E. Doran, A.E. Stuchbery, H.H. Bolotin, A.P. Byrne and G.J. Lampard, Phys. Rev. C **40**, 2035 (1989)
33. S. Raman, C.H. Malarkey, W.T. Milner, C.W. Nestor Jr., and P.H. Stelson, At. Data Nucl. Data Tables **36**, 1 (1987)
34. W. Greiner, Nucl. Phys. **80**, 417 (1966)
35. J.N. Ginocchio, W. Frank and P. von Brentano, Nucl. Phys. A **541**, 211 (1992)
36. K.S. Krane and R.M. Steffen, Phys. Rev. **C**2, 724 (1970)
37. J.G. Hisch, private communication
38. V. Velasquez, J.G. Hirsch, Y. Sun, M.W. Guidry, Nucl. Phys. A, in press.
39. A.E. Stuchbery and E. Besakova, Phys. Rev. Lett., in press.